Energy Reports 8 (2022) 10183–10192

Contents lists available at ScienceDirect

Energy Reports

journal homepage: www.elsevier.com/locate/egyr

Analysis of combined low-level indicators for the hot-season performance of roof components

Chiara Lodi [a], Alberto Muscio [a,*], Paolo Tartarini [a], Hashem Akbari [b]

[a] University of Modena and Reggio Emilia, Modena, Italy
[b] Concordia University, Montreal, Canada

ARTICLE INFO

Article history:
Received 15 February 2022
Received in revised form 24 June 2022
Accepted 30 July 2022
Available online xxxx

Keywords:
Albedo
Building cooling
Periodic thermal transmittance
R-value
Solar absorptance
Solar factor
Solar reflectance
Solar transmittance factor
Solar transmittance index
U-value

ABSTRACT

A single performance indicator, the solar transmittance factor (STF), has been proposed in previous works, together with the derived solar transmittance index (STI). It is aimed at evaluating the summer performance of the roofing system and allowing the selection of the most effective mix of surface and mass properties. It is easily calculated from low-level indicators such as U-value, module of periodic thermal transmittance, and solar reflectance. In the present work, the correlation between STF and the cooling energy demand, integrated over a reference period, was studied, as well as the peak of ceiling temperature increase with respect to the indoor temperature, relevant for thermal comfort. In particular, the thermal behavior of different roof types with variable insulation was calculated numerically by TRNSYS 17 for a wide set of locations and environmental conditions. Unlike other commonly used indicators, to which the analysis has been extended, a strong correlation with STF was found for both cooling energy demand and ceiling temperature rise.

1. Introduction

The forecast of the energy needs for air conditioning, *e.g.* to rate the energy performance of a building or to analyze the cost-effectiveness of an energy retrofit action, often requires a dynamic simulation. This is typically calculated with a time step of an hour or less and takes into account a wide range of parameters, related to the place of installation with its climate and to the seasonal and/or daily cycle of meteorological variables, as well as to the thermal properties of the building envelope. The latter consist of the insulation and inertia of the building components and their surface properties relevant to solar gains, as well as the characteristics of the transparent components and their shielding. Other aspects to consider are the response of the air conditioning system as controlled by building automation devices and the complex interaction between climate, characteristics of the inhabited space, air conditioning system and usage profile. Dynamic simulation, however, is not the most common design approach: the energy needs for air conditioning are often calculated with simplified procedures, *e.g.* in terms of a quasi-stationary thermal balance calculated on a daily or monthly basis, in which the fluctuation of meteorological parameters and the dynamic interaction between the building envelope and the air conditioning system are neglected. Moreover, due to different climatic conditions and usage profile, a significant discrepancy may however arise between the numerically calculated and actual building performances, so complex calculation methods are not necessarily justified. Moreover, the actual climatic conditions and the building use profile can be very different from the reference ones considered in the simulation, therefore a significant discrepancy may arise between the numerically calculated building performance and the real one. As a result, complex calculation methodologies are not necessarily justified.

A statement made by Mahdavi and reported in Kabre (2010) is that *building component properties may be interpreted as "low level" performance indicators, whereas room performance descriptions may be interpreted as "high-level" behavioral properties*. The first category includes several easy-to-use indicators such as: the overall heat transfer coefficient or thermal transmittance (U-value) or its inverse, the thermal resistance (R-value); the modulus of the periodic thermal transmittance or the closely related attenuation factor and time shift; the solar reflectance or albedo, and the solar reflectance index SRI (see (Muscio and Akbari, 2017; Akbari et al., 2021) for a brief review). These can be rated by manufacturers or easily calculated by construction professionals according to standard methods; therefore, in building regulations they are often exploited to encourage energy efficient design by defining specific requirements that are easily verifiable.

* Corresponding author.
E-mail address: alberto.muscio@unimore.it (A. Muscio).

https://doi.org/10.1016/j.egyr.2022.07.173

On the other hand, the actual performance of a building depends on the complex interaction of multiple properties of the building components, of which it may not be easy to identify a cost-effective combination, especially with reference to the thermal behavior in the hot season. The second category of *room performance descriptions* generally requires a comprehensive modeling of the overall building behavior, referring to environmental conditions that depend on the location, the season and the daily cycle, and which often fall within the aforementioned field of dynamic simulation. For example, non-dimensional thermal performance indicators involving the behavior of the whole building were proposed by Pisello et al. (2012) in terms of the thermal deviation indexes (TDI), to be calculated by a complete dynamic simulation. Intermediate approaches have been proposed with the overall thermal transfer value (OTTV) for commercial buildings (Hong Kong Building Authority, 1995) and the residential thermal transfer value (RTTV) for residential buildings (Hong Kong Building Department, 2014). These are aimed to forecast the average heat gain through the building envelope over a wide time period. Indeed, cooling loads and electricity consumption in Hong Kong were found to be related to OTTV in terms of a simple two-parameter linear regression equation (Lam et al., 2005). Under the pressure of the various Energy Performance of Buildings Directives (EPBD) (European Parliament and Council, 2002, 2010, 2018), rating programs have also been developed in all European Union countries, considering the overall energy needs for heating, cooling and other services calculated over a season or even the whole year.

While providing reasonably objective results, high-level behavioral properties or overall building performance indicators do not seem practical for selecting individual building components: skilled professionals, validated software tools, and time-consuming simulation work are required, which may be discouraging in cases of design of small buildings or implementation of simple energy retrofit actions. While the combined effects of mass and surface properties on energy performance and the indoor comfort in the hot season can be effectively estimated by means of numerical techniques (Barrios et al., 2012, 2016) or even by experimental ones (Cheng et al., 2013), complex assessment approaches are seldom useful for quick selection of the optimal building component as they are out of reach for many construction professionals.

A satisfactory trade-off between ease of use and accuracy of results could be achieved by the adoption of combined performance indicators, resulting from the combination of a set of simpler low-level indicators that take into account all the heat transfer processes affecting a building component. This would allow selecting with relative ease the most effective mix of surface and mass properties. It is indeed difficult to identify such a mix by looking at the different performance parameters separately. In fact, in the hot season, a roof with high thermal inertia but a dark surface can behave like a roof with relatively low inertia but with a solar reflective surface. A highly reflective surface would almost nullify the effects of the solar cycle, but it is not easy to preserve due to ageing and dust deposition. Moreover, a highly reflective surface is generally white, but different colors may be required, even if less reflective, due to architectural or landscape conservation constraints; in these cases, the weight of thermal inertia increases together with that of thermal insulation. Even so, pursuing a high thermal inertia can conflict with seismic requirements and costs if achieved by adopting a high mass, while it can impact durability and fire risk if achieved using high capacity materials such as wood fiber. In view of all that, a combined performance indicator, the solar transmittance factor (STF), was proposed in previous works (Muscio and Akbari, 2017; Akbari et al., 2021) together with the derived solar transmittance index (STI). It consists of a combination of standard low-level indicators such as U-value, module of periodic thermal transmittance, and solar reflectance. In the present work, the thermal behavior of different roof types with variable insulation was calculated numerically by TRNSYS 17 for a wide set of locations and environmental conditions. The correlation of STF with the cooling energy demand, integrated over a reference period, was analyzed, as well as with the ceiling temperature increase with respect to the indoor temperature, relevant for thermal comfort. The correlation was investigated also for other commonly used indicators such as U-value, modulus of the periodic thermal transmittance, and solar factor, to which the analysis was extended.

2. Formulation of STF and other performance indicators

In the French legislation in force in some locations with a warm climate, values not to be exceeded are prescribed for the solar factor (*facteur solaire*) of roofs or walls (République Française, 2017). Similarly to the solar factor for glazed components, it is defined as the ratio between the density of solar heat flux q_{sol} (W/m^2) passing through a component and the solar irradiance I_{sol} (W m^{-2}) incident on the outer surface of the component:

$$S_p = \frac{q_{sol}}{I_{sol}} \tag{1}$$

The solar factor of opaque building components S_p ($0 < S_p < 1$) is calculated according to the simplified formula

$$S_p = C_m \cdot U \cdot R_{se} \cdot \alpha_{sol} \equiv C_m \cdot U \cdot R_{se} \cdot (1 - \rho_{sol}) \tag{2}$$

where

C_m coefficient of reduction due to the possible presence of a ventilated external sunshield or a similar solar protection ($0 \le C_m \le 1$, $C_m = 1$ without sunshield)

R_{se} surface thermal resistance at the external surface, in summer calculated for a wind speed of 1 (m^{2}K W^{-1})

U overall heat transfer coefficient, o U-value, of the component, including the external and internal surface thermal resistances (W m^{-2} K^{-1})

α_{sol} solar radiation absorption coefficient of the external surface of the component ($0 < \alpha_{sol} < 1$)

ρ_{sol} solar reflectance of the external surface of the component ($0 < \rho_{sol} < 1$)

S_p seems adequate for lightweight roofs, whereas it may not catch capacitive effects in heavy roof.

A significant contribution in the field of combined performance indicators was brought by the thermal performance index (TPI) (Chandra, 1980). More specifically, the impact of the internal surface temperatures T_{si} (°C) on thermal comfort in unconditioned buildings with free floating indoor temperature T_i was emphasized by correlating TPI to the excess of the T_{si} peak above a reference value of 30 °C; the rating 100 corresponds to an excess of 8 °C (the lower the better). For conditioned buildings, T_i is assumed to be maintained constant at 25 °C, and TPI is correlated to the peak of indoor heat gain q_i (W m^{-2}): the rating 100 corresponds to a peak of 40 (kcal m^{-2} h^{-1}), that is 46.52 (W m^{-2}). In this case, for constant indoor temperature T_i (° C) and assigned inside surface thermal resistance R_{si} (m^{2}K W^{-1}), T_{si} and q_i are directly correlated between themselves:

$$q_i = \frac{T_{si} - T_i}{R_{si}} \tag{3}$$

It is reported in Kabre (2010) that TPI values for typical roof sections and reference ambient conditions are included in the Bureau of Indian Standards.

For an energy saving perspective such as that of this paper, the conditioned building case is the most relevant one. In this case, TPI can be calculated for a single component, disregarding the characteristics of the building in which the component is installed. Nonetheless, a numerical calculation is required in view of the variability of outdoor ambient conditions, and correction factors are needed for ambient conditions different from the reference one. Moreover, the reference peak heat gain for TPI = 100 is arbitrary. The approach was improved through the "new" thermal performance index (TPI*) proposed in Kabre (2010), which is focused on roof components and their inside surface temperature, that is the ceiling temperature. This temperature is calculated by a "harmonic" analytical approach, fundamentally equivalent to the thermal quadrupole method specified in ISO (2017): the daily cycle of the sol-air temperature is developed in a series of sinusoidal harmonics with decreasing period. Following a widely used approximation, harmonics other than the base one with period 24 h are neglected since they are quickly damped through the building component and do not affect significantly the inside surface temperature. TPI* is evaluated from the elevation of the ceiling temperature T_{si} with respect to the mean (monthly) outdoor temperature $T_{e,m}$(°C). In particular, TPI* (the higher the better) is the difference between elevation of the ceiling temperature in the worst case of a galvanized iron roof and that in the considered case, divided by the difference of the temperature elevation in the worst case and that in a reference acceptable case:

$$\begin{aligned} TPI* &= 100 \cdot \frac{\left(T_{si,max} - T_{e,m}\right) - \left(T_{si} - T_{e,m}\right)}{\left(T_{si,max} - T_{e,m}\right) - \left(T_{si,min} - T_{e,m}\right)} \\ &\equiv 100 \cdot \frac{T_{si,max} - T_{si}}{T_{si,max} - T_{si,min}} \end{aligned} \tag{4}$$

As shown in the previous formula, $T_{e,m}$ can eventually be eliminated in the calculation. It can still surface, however, in the temperature-dependent terms from which T_{si} is calculated and, above all, in the acceptable ceiling temperature $T_{si,min}$. This is calculated from the adaptive psycho-physiological empirical model of thermal perception formulated by (Auliciems, 1982), in which the indoor temperature $T_{i,N}$ (°C) corresponding to thermal neutrality, *i.e.* to the best comfort condition, is related to the mean monthly outdoor temperature as people would try to attain thermal neutrality by modifying clothing, air movement, etc.:

$$T_{i,N} = 17.6 + 0.31 \cdot T_{e,m} \tag{5}$$

According to ISO (2005), the operative (*i.e.* perceived) indoor temperature is a weighted average of indoor air temperature T_{ai} (°C) and mean radiant temperature T_{mr} (° C) of the internal surfaces.

$$T_i = p \cdot T_{ai} + (1 - p) \cdot T_{mr} \tag{6}$$

T_{mr} is the mean temperature on the internal surfaces, weighted by the view factors associated to the solid angles subtended by those surfaces with respect to the position in which thermal comfort is evaluated. The weight p decreases with decreasing air velocity, which should be as low as possible in a comfortable environment. For air velocity not higher than 0.2 m/s, $p = 0.5$ and the indoor temperature is the arithmetic mean of air and mean radiant temperatures; p increases to 0.6 for a higher air velocity but not more than 0.6 m/s, and to 0.7 for furtherly higher velocity up to 1.0 m/s. In Kabre (2010), p is set equal to 1/3 as a warm climate is considered, in which the lighter clothing is supposed to increase the relative weight of T_{mr}. Again in Kabre (2010), a reasonable situation is considered, in which all surfaces apart from the ceiling are about at the air temperature, so that:

$$T_{mr} = F \cdot T_{si} + (1 - F) \cdot T_{ai} \tag{7}$$

where $F = \omega/4\pi$ is the view factor associated to the solid angle ω (rad) subtended by the ceiling.

Combining Eqs. (5)–(7) and solving with respect to T_{si}, one eventually obtains the acceptable ceiling temperature that ensures thermal neutrality as a function of the mean monthly outdoor temperature:

$$\begin{aligned} T_{si,min} &= T_{ai} + \frac{17.6 + 0.31 \cdot T_{e,m} - T_{ai}}{F \cdot (1 - p)} \\ &\approx \frac{17.6}{F \cdot (1 - p)} + \left[1 - \frac{0.69}{F \cdot (1 - p)}\right] \cdot T_{e,m} \end{aligned} \tag{8}$$

The final approximation is that used in Kabre (2010) for TPI* calculation, assuming that $T_{ai} \approx T_{e,m}$ in view of room ventilation with outdoor air. In a sealed, air-conditioned room, the value of T_{ai} is that set by the air conditioning system. The solid angle ω can be calculated by several methods, also depending on the position in the room. For example, a chart or an online calculator are available for a standing person under a flat horizontal ceiling (Howell, 2022). The approach is indeed interesting and reasonably simple. Eq. (8) is analogous to the formula for calculation of the solar reflectance index (SRI) (ASTM, 2019; Muscio, 2018).

A similar yet furtherly simplified approach was followed in the development of the solar transmittance factor (STF) and the derived solar transmittance index (STI) (Muscio and Akbari, 2017; Akbari et al., 2021). As already stated, STF is a combined performance indicator resulting from the combination of a set of simpler low-level indicators.

In brief, while the outer surface of a roof component is subjected to the daily cycle of solar irradiance I_{sol} (W m^{-2}), the forcing cycle is that of the sol-air temperature $T_{sol-air}$ (°C), obtained increasing the outdoor temperature T_e by an amount that takes into account the effects of the absorbed solar radiation. $T_{sol-air}$ follows the I_{sol} cycle, which can be decomposed in a Fourier series made of the sum of an infinite set of sines or cosines, with base period $t_0 = 24$ h:

$$\begin{aligned} T_{sol-air}(t) \cong\ & T_{e,m} + R_{se} \cdot (1 - \rho_{sol}) \cdot I_{sol,m} + \\ & + R_{se} \cdot (1 - \rho_{sol}) \cdot \sum_{n=1}^{\infty} I_{sol,n} \cdot \left(n \cdot 2\pi \cdot \frac{t}{t_0} + \psi_n\right) \end{aligned} \tag{9}$$

$I_{sol,m}$ (W m^{-2}) is the daily average value of the solar irradiance; $I_{sol,n}$ (W m^{-2}) and ψ_n (rad) are amplitude and phase of the *n*th harmonic term of the I_{sol} cycle, respectively. Especially in a humid and polluted atmosphere, the oscillation amplitude of T_e is relatively weak over urban and suburban areas, which include most of the building lots, therefore it has been neglected and the daily average value of the outdoor temperature $T_{e,m}$(°C) has been considered.

The sol-air temperature cycle propagates through the roof component and eventually contributes to the heat flux entering the internal ambient, which has an average density $q_{i,m}$ (W m^{-2}) controlled by the U-value:

$$q_{i,m} \cong U \cdot \left(T_{e,m} - T_i\right) + U \cdot R_{se} \cdot (1 - \rho_{sol}) \cdot I_{sol,m} \tag{10}$$

This is the daily average cooling power to be supplied by the AC system to offset the heat transmitted through the considered building component. Some supplementary power, however, is required to counter the oscillating part of the sol-air temperature, which peaks at noon and affects the ceiling radiant temperature. In this regard, the length of penetration of the oscillating terms of $T_{sol-air}$ decreases with their order n. Therefore, the analysis can be limited to the first-order term (n = 1), the one yielding the most

significant effects in the indoor space (ISO, 2017; Muscio and Akbari, 2017). As a result, the oscillating component of the entering heat flux is also harmonic. Its amplitude $q_{i,n=1}$ (W m^{-2})(W m^{-2}) is correlated to the amplitude of the first order component of solar irradiance $I_{sol,n=1}$ through the modulus of the (complex) periodic thermal transmittance Y_{ie} (W m^{-2} K^{-1}):

$$q_{i,n=1} \leq Y_{ie} \cdot R_{se} \cdot (1 - \rho_{sol}) \cdot I_{sol,n=1} \quad (11)$$

Y_{ie} is calculated according to ISO (2017) from the layer structure of the considered component and the thermophysical properties of the layer materials (thermal conductivity, density and specific heat). It is a representation of the heat flow cycle produced at the inner surface by a temperature oscillation at the outer side while the indoor temperature is maintained constant. The higher is thermal inertia, the lower is Y_{ie}, which is always lower than U.

The solar irradiance cycle can also be approximated by a sine oscillation, in which the average value of the irradiance is made equal to its amplitude of oscillation ($I_{sol,m} \approx I_{sol,n=1}$). The effect of using a sinusoidal boundary conditions was found to be small and generally cautionary (Gasparella et al., 2011). As a result, the peak cooling power to be provided by an AC system is calculated by the combination of Eq. (11) with Eq. (10), where the indoor temperature T_i is assumed to be kept relatively close to $T_{e,m}$ by an ideal air conditioning system ($T_i \approx T_{e,m}$) in view of the thermal neutrality concept represented by Eq. (5):

$$\begin{aligned} q_{i,peak} = q_{i,m} + q_{i,n=1} \leq U \cdot R_{se} \cdot (1 - \rho_{sol}) \cdot I_{sol,m} \\ + Y_{ie} \cdot R_{se} \cdot (1 - \rho_{sol}) \cdot I_{sol,n=1} \approx \\ \approx (U + Y_{ie}) \cdot R_{se} \cdot (1 - \rho_{sol}) \cdot I_{sol,m} \end{aligned} \quad (12)$$

A comprehensive indicator has eventually surfaced. This was called 'solar transmittance factor' (STF) (Muscio and Akbari, 2017), the lower the better. It includes both the radiative properties at the external surface and the thermo-physical properties of the materials under the surface:

$$STF = \frac{q_{i,peak}}{I_{sol,m}} = (U + Y_{ie}) \cdot R_{se} \cdot (1 - \rho_{sol}) \quad (13)$$

STF is plotted in Fig. 1 versus the whole spectrum of values of the solar reflectance ρ_{sol}. Two different U-values of 0.3 W m^{-2} K^{-1}, corresponding to a well-insulated roof or wall, and 0.8 W m^{-2} K^{-1}, often used to distinguish between insulated and non-insulated building components, have been considered. For the Y_{ie}/U ratio, *i.e.* the so-called decrement factor, values have been considered from 0.25, corresponding to a massive component with high thermal inertia, to 1.00, corresponding to a lightweight component with negligible inertia.

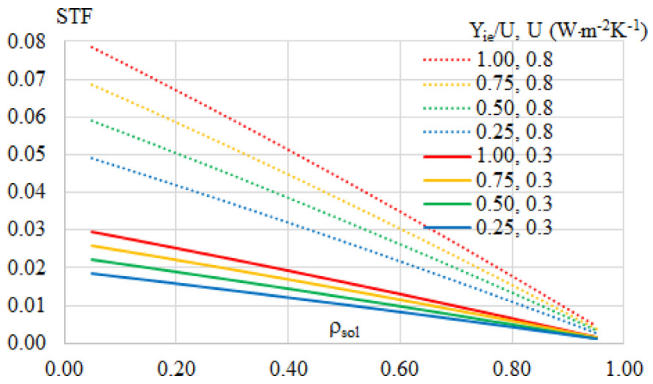

Fig. 1. Solar transmittance factor (STF) versus solar reflectance ρ_{sol}, for two different values of U (0.8 W m^{-2} K^{-1} for an almost uninsulated component and 0.3 W m^{-2} K^{-1} for a well-insulated component) and several values of Y_{ie}/U (from 1 for a lightweight component with very low mass down to 0.25 for a massive component).

In view of Eq. (3), from the peak of entering heat flux density, one can estimate the peak of radiant temperature of the ceiling:

$$T_{si,peak} - T_i = R_{si} \cdot q_{i,peak} \approx R_{si} \cdot STF \cdot I_{sol,m} \quad (14)$$

STF would tend to very low values for high performance building components, so it does not seem an effective choice for a performance indicator as it would not allow differentiating alternative solutions. An analogous issue was considered in Kabre (2010) while defining the 'new' thermal performance index TPI*. The same approach of TPI*, maybe inspired by that for calculation of SRI (ASTM, 2019), has been applied in an even more practical way, moreover independent of the local weather conditions, through the solar transmittance index (STI) proposed in Muscio and Akbari (2017):

$$STI = 100 \cdot \frac{STF_{worst} - STF_{tested}}{STF_{worst} - STF_{optimal}} \quad (15)$$

STI represents the percent fraction of the peak heat flux density transmitted inside in the worst reference case, which is cancelled by means of the considered building solution, evaluated in excess to the optimal reference case. An issue still under investigation is the choice of the worst and optimal reference values of STF, preliminary addressed in Muscio and Akbari (2017) but not deepened here. Instead, in this paper the focus is on the correlation of cooling heat load and ceiling overheating with STF in a variety of climate conditions. The correlation with U-value, Y_{ie} and the solar factor as defined in Eqs. (1)–(2) is also considered.

Table 1
Considered locations and reference data for the hot season period.

Location	Country	Climate classification	Latitude	Average temperature (°C)	Peak temperature (°C)	Average irradiance (W m^{-2})
Beijing	China	D (Dwa = Cold, dry winter, hot summer)	39°54′27″ N	24.57	37.40	177
Brasilia	Brazil	A (Aw = Tropical savanna climate with dry-winter)	15°46′47″ S	21.38	30.90	206
Cairo	Egypt	B (Bwh = tropical and subtropical desert climate)	30°00′20″ N	27.24	39.15	312
Montreal	Canada	D (Dfb = warm-summer humid continental climate)	45°30′32″ N	19.07	32.15	243
Perth	Australia	C (Csa = hot-summer Mediterranean climate)	31°57′13″ S	22.79	39.15	323
Rome	Italy	C (Csa = hot-summer Mediterranean climate)	41°53′31″N	22.37	34.25	278

Considered three-month hot season period: 20/5–20/8 (Beijing, Cairo, Montreal, Rome) or 20/11–20/02 (Brasilia, Perth).

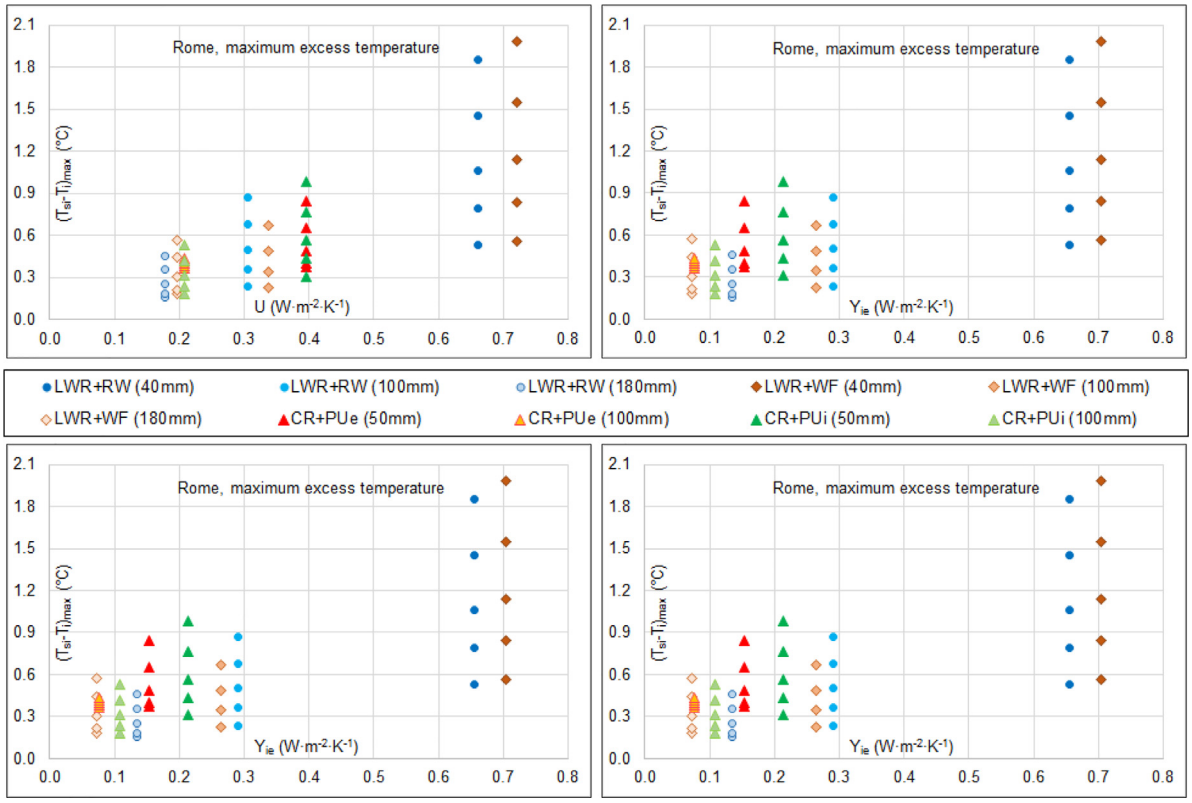

Fig. 2. Increase of the ceiling temperature T_{si} above the indoor temperature T_i for different roofing solutions, insulation thickness and surface properties, in Rome. The U-value and the periodic transmittance Y_{ie} value are reported in Table 2.

None of the considered indicators allows assessing the performance of roofing solutions based on phase change materials as proposed in Piselli et al. (2019), Triano-Juárez et al. (2020): solar factor does not take into account capacitive effects, whereas a kind of equivalent periodic thermal transmittance should be identified to allow using STF. Instead, most of the indicators can be applied to angular-selective and retro-reflective materials (Akbari and Touchaei, 2014; Manni and Nicolini, 2021) as long as a stable equivalent albedo can be identified in the reference solar irradiance conditions.

3. Model and methods

In the present work, the correlation has been studied between STF and both the demand for cooling energy and the peak of the ceiling temperature increase with respect to the indoor temperature. The same approach already used in Akbari et al. (2021) has been followed: the thermal behavior of different roof types with variable insulation has been calculated numerically by TRNSYS 17. A much wider set of locations and environmental conditions have been considered, in both the northern and southern hemispheres, in order to make evident the robustness of the proposed indicator. The solar factor as defined in Eq. (2) has also been analyzed, as well as simpler indicators such as U-value, periodic thermal transmittance Y_{ie}, solar reflectance and SRI.

In the simulation model, a 3 m high single-zone building with a roof area of 3 m × 3 m has been created, in which a constant inside air temperature of 26 °C was set. All surfaces, except the roof, have been set adiabatic as the focus is on the thermal behavior of the roof component only. Most importantly, the three hottest months in the year have been considered in a wide range of locations and environmental conditions. The locations are summarized in Table 1, where they are classified according to the Köppen–Geiger climate classification (Beck et al., 2018).

The analysis extended from a lightweight wooden roof, for which different types and levels of insulation have been considered, to a concrete roof with different levels and also different positions of the insulation layer (see Table 2). These are roof types that can commonly be found in all locations where the simulations have been located, and all types have been simulated in all locations. For each roofing solution, five different values have been considered for the solar reflectance $\rho_{sol} = 1 - \alpha_{sol}$: 0.1 (representative of a dark black surface), 0.3 (colored surface with relatively dark color), 0.5 (light colored surface), 0.65 (aged white 'cool' surface) and 0.8 (bright white 'cool' surface). For all cases, a high-emissivity surface has been assumed, as common with non-metallic materials, with thermal emittance 0.9. Intermediate wind conditions have also been considered, resulting in R_{se} between 0.055 and 0.057 $m^2\,K\,W^{-1}$, depending on the surface temperature. The calculated values of STF and of the solar factor S_p are collected in Table 3 and Table 4, respectively.

4. Analysis of results

As easily expectable, a large scattering is evident for the maximum increase in the ceiling temperature T_{si} above the indoor temperature T_i with respect to both the U-value and the periodic thermal transmittance Y_{ie}. This is shown in Fig. 2 for Rome, as calculated in the reference hot season period for all the roofing solutions considered, but it is similar for all the other locations. The same occurs with the cooling energy demand cumulated over the reference hot season period, shown in Fig. 3. In this regard, the hours with negative (*i.e.* outgoing) heat flow are neglected in order to catch the heat load relevant for the air conditioning. Solar reflectance and solar reflectance index (SRI), which only take into

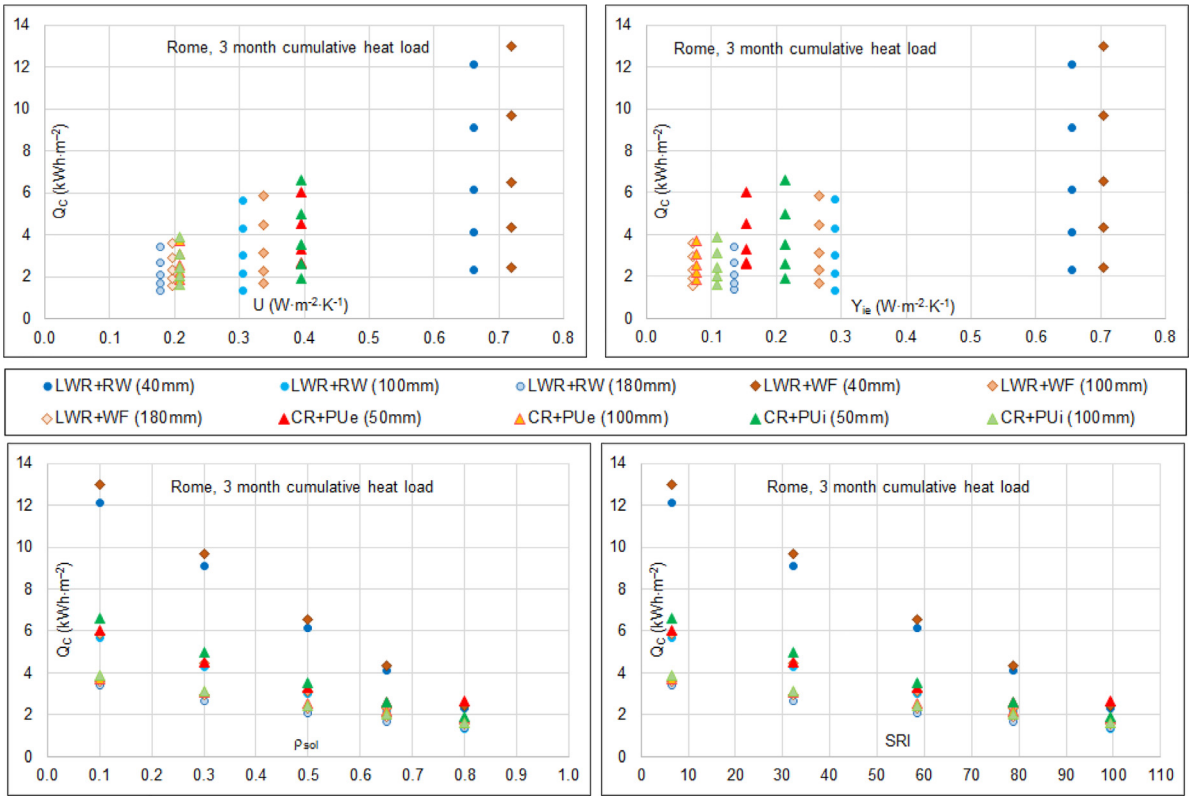

Fig. 3. Cooling energy demand cumulated over the reference hot season period for different roofing solutions, insulation thickness and surface properties, in Rome. U-value and periodic transmittance Y_{ie} are reported in Table 2.

Table 2
Roofing solutions considered in the numerical simulation.

Roof type	Roof layers	Conductivity (W m^{-1} K^{-1})	Density (kg m^{-3})	Specific heat (kJ kg^{-1} K^{-1})	Thickness (mm)
Light wooden roof + rock wool (low density) insulation LWR+RW	Waterproofing membrane	0.26	1300	1	1
	Wooden panel	0.12	450	2.7	10
	Rock wool (RW) panel	0.034	95	1.03	0; 40; 100; 180
	Wooden panel	0.12	450	2.7	10
	U-value (W m^{-2} K^{-1})	2.980; 0.661; 0.305; 0.178 (w/ null, 40 mm, 100 mm, 180 mm insulation)			
	Y_{ie} (W m^{-2} K^{-1})	2.969; 0.655; 0.291; 0.135 (w/ null, 40 mm, 100 mm, 180 mm insulation)			
Light wooden roof + wood fiber (low density) insulation LWR+WF	Waterproofing membrane	0.26	1300	1	1
	Wooden panel	0.12	450	2.7	10
	Wood fiber (WF) panel	0.038	120	2.4	0; 40; 100; 180
	Wooden panel	0.12	450	2.7	10
	U-value (W m^{-2} K^{-1})	2.980; 0.720; 0.337; 0.197 (w/ null, 40 mm, 100 mm, 180 mm insulation)			
	Y_{ie} (W m^{-2} K^{-1})	2.969; 0.704; 0.265; 0.072 (w/ null, 40 mm, 100 mm, 180 mm insulation)			
Concrete roof + polyurethane foam insulation, external CR+PUe	Waterproofing membrane	0.26	1300	1	1
	Polyurethane (PU) panel	0.022	36	1.45	0; 50, 100
	Reinforced concrete	1.49	2200	0.88	50
	Concrete	1.61	2200	1	60
	Plaster	0.8	1600	1	15
	U-value (W m^{-2} K^{-1})	4.318; 0.395; 0.208 (w/ null, 50 mm, 100 mm insulation)			
	Y_{ie} (W m^{-2} K^{-1})	2.855; 0.153; 0.077 (w/ null, 50 mm, 100 mm insulation)			
Concrete roof + polyurethane foam insulation, internal CR+PUi	Waterproofing membrane	0.26	1300	1	1
	Reinforced concrete	1.49	2200	0.88	50
	Concrete	1.61	2200	1	60
	Polyurethane (PU) panel	0.022	36	1.45	0; 50, 100
	Plaster	0.8	1600	1	15
	U-value (W m^{-2} K^{-1})	4.318; 0.395; 0.208 (w/ null, 50 mm, 100 mm insulation)			
	Y_{ie} (W m^{-2} K^{-1})	2.855; 0.214; 0.108 (w/ null, 50 mm, 100 mm insulation)			

account surface properties, are also not appropriate indicators as dispersion increases.

Instead, a clear trend is evident in most cases with respect to both STF and S_p. (Figs. 4–5). Aside from Montreal, the location with the highest latitude and coldest climate, the maximum increase of the ceiling temperature T_{si} above the indoor temperature T_i shows a strong correlation with STF (Fig. 4). There is a little more scattering than for S_p, however the correlation is still fair

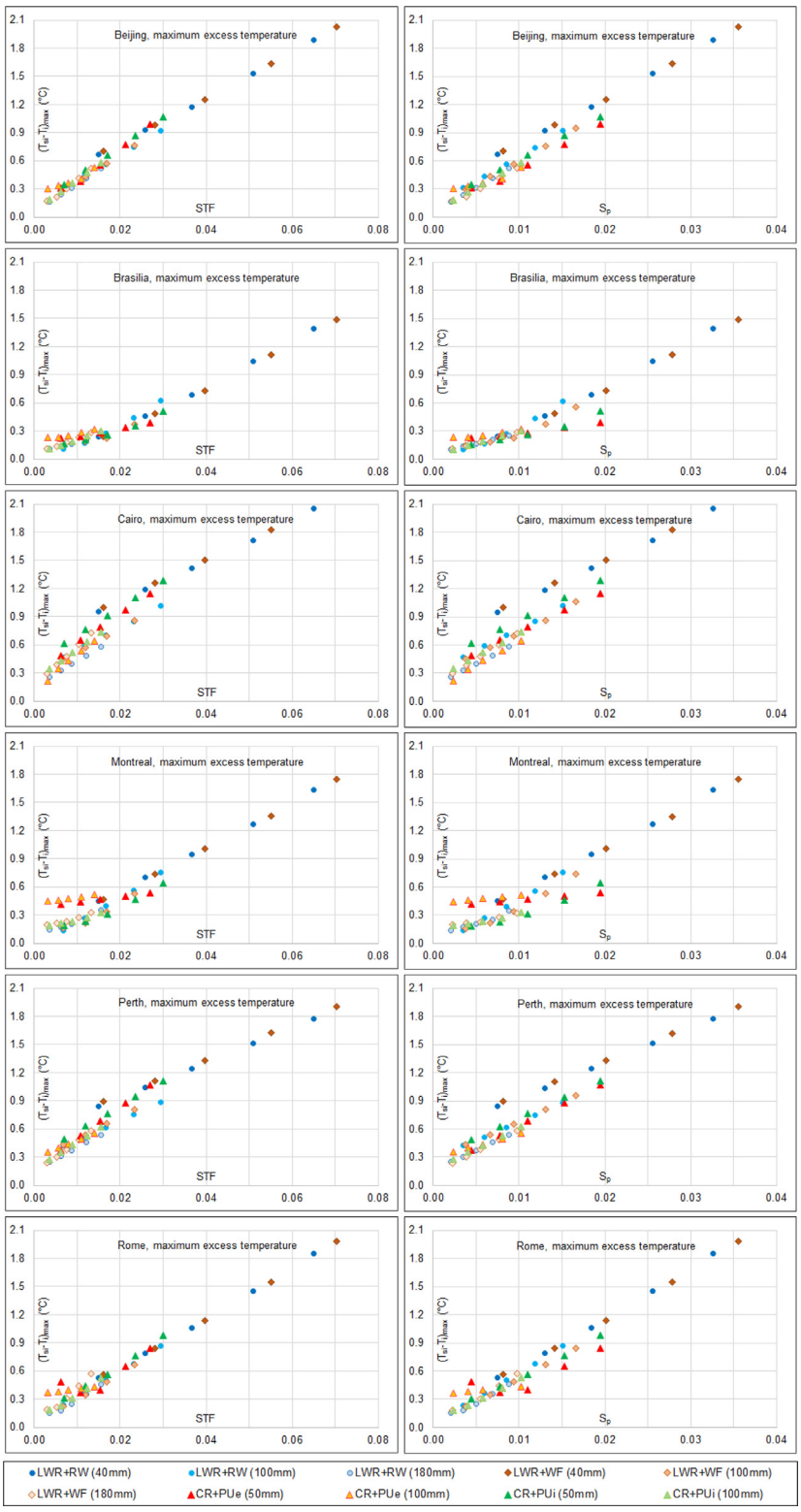

Fig. 4. Increase of the ceiling temperature T_{si} above the indoor temperature T_i for different roofing solutions and insulation thickness in several locations. STF values are reported in Table 3, S_p values are reported in Table 4.

in most cases. The correlation becomes good with both STF and S_p for the cooling energy demand cumulated over the reference hot season period (Fig. 5), again with some more scattering for Montreal.

In brief. The daily average ceiling temperature increases with the solar factor S_p. This takes into account thermal insulation and surface properties, and it is a performance parameter relevant to the average energy needs for air conditioning. On the other hand, the peak of ceiling temperature seems to depend on both S_p and STF, which takes into account also thermal inertia. It is relevant to energy need as well as to thermal comfort, more specifically to the maximum level of thermal discomfort.

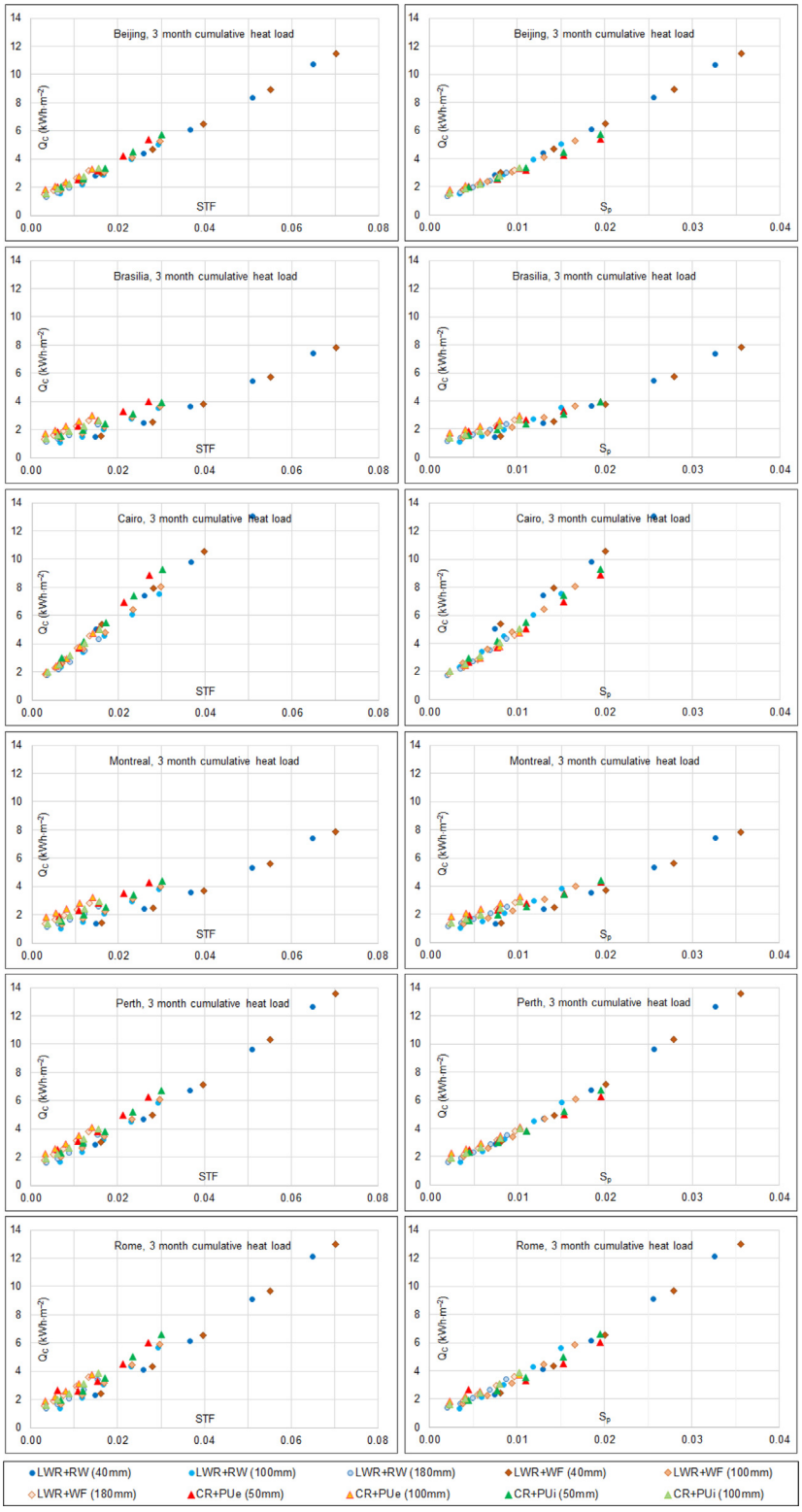

Fig. 5. Cooling energy demand cumulated over the reference hot season period for different roofing solutions and insulation thickness in different locations. STF values are reported in Table 3, S_p values are reported in Table 4.

5. Concluding remarks

The correlation between STF and the maximum increase of the ceiling temperature above the indoor temperature has been investigated numerically. The correlation between STF and the cooling energy demand cumulated over a three-month period of the hot season has also been analyzed. Compared to previous work, the analysis has been extended to several worldwide locations, with different latitudes and climates, and other indicators have been added to the analysis such as the solar factor S_p, which takes into account the insulation but not the inertia of the opaque roof component. A lightweight wooden roof has been

Table 3
Solar transmittance factor (STF) for the considered roofing solutions with different values of the solar reflectance.

Roof type and insulation	U (W m^{-2} K^{-1})	Y_{ie} (W m^{-2} K^{-1})	ρ_{sol}				
			0.80	0.65	0.50	0.30	0.10
			Solar transmittance factor (STF)				
LWR	2.980	2.969	0.067	0.117	0.166	0.230	0.294
LWR+RW 040 mm	0.661	0.655	0.015	0.026	0.037	0.051	0.065
LWR+RW 100 mm	0.305	0.291	0.007	0.012	0.017	0.023	0.029
LWR+RW 180 mm	0.178	0.135	0.004	0.006	0.009	0.012	0.015
LWR+WF 040 mm	0.720	0.704	0.016	0.028	0.040	0.055	0.070
LWR+WF 100 mm	0.337	0.265	0.007	0.012	0.017	0.023	0.030
LWR+WF 180 mm	0.197	0.072	0.003	0.005	0.008	0.010	0.013
CR	3.896	2.855	0.076	0.133	0.188	0.261	0.333
CR+PUe 050 mm	0.395	0.153	0.006	0.011	0.015	0.021	0.027
CR+PUe 100 mm	0.208	0.077	0.003	0.006	0.008	0.011	0.014
CR+PUi 050 mm	0.395	0.214	0.007	0.012	0.017	0.024	0.030
CR+PUi 100 mm	0.208	0.108	0.004	0.006	0.009	0.012	0.016

Table 4
Solar factor (S_p) for the considered roofing solutions with different values of the solar reflectance.

Roof type and insulation	U (W m^{-2} K^{-1})	ρ_{sol}				
		0.80	0.65	0.50	0.30	0.10
		Solar factor (S_p)				
LWR	2.980	0.034	0.059	0.083	0.115	0.147
LWR+RW 040 mm	0.661	0.007	0.013	0.018	0.026	0.033
LWR+RW 100 mm	0.305	0.003	0.006	0.009	0.012	0.015
LWR+RW 180 mm	0.178	0.002	0.004	0.005	0.007	0.009
LWR+WF 040 mm	0.720	0.008	0.014	0.020	0.028	0.036
LWR+WF 100 mm	0.337	0.004	0.007	0.009	0.013	0.017
LWR+WF 180 mm	0.197	0.002	0.004	0.005	0.008	0.010
CR	3.896	0.044	0.077	0.109	0.151	0.192
CR+PUe 050 mm	0.395	0.004	0.008	0.011	0.015	0.019
CR+PUe 100 mm	0.208	0.002	0.004	0.006	0.008	0.010
CR+PUi 050 mm	0.395	0.004	0.008	0.011	0.015	0.019
CR+PUi 100 mm	0.208	0.002	0.004	0.006	0.008	0.010

considered, with different types and levels of insulation, as well as a massive concrete roof with different levels and positions of the insulation layers, so as to have a large variety of STF and S_p values. A strong correlation with STF was found for both ceiling temperature increase and cooling energy demand in nearly all locations considered. In fact, a fair correlation was also observed with S_p, but with some more scattering for the peak temperature of the ceiling. A validation has not yet been possible as suitable data have not been found in the literature due to lack of some crucial information on documented test cases. Therefore, experiments aimed at the validation in actual conditions are planned, based on the accurate characterization of surfaces (solar reflectance, thermal emittance), bulk materials (specific heat, thermal conductivity), ambient conditions (wind velocity, solar irradiance, etc.) and the comparison of measured temperatures with simulated data in different ambient conditions.

The next step will be to investigate the causes of some discrepancies, however moderate, that have emerged for selected locations and types of building components. Furthermore, and above all, the development of the derivative solar transmittance index (STI) will be carried out as this is expected to provide a more explicit indicator for the energy and comfort rating of opaque building components.

CRediT authorship contribution statement

Chiara Lodi: Methodology, Investigation, Writing – original draft, Writing – review & editing. **Alberto Muscio:** Conceptualization, Methodology, Investigation, Writing – original draft, Writing – review & editing. **Paolo Tartarini:** Investigation, Writing – original draft. **Hashem Akbari:** Conceptualization, Writing – review & editing.

Declaration of competing interest

The authors declare that they have no known competing financial interests or personal relationships that could have appeared to influence the work reported in this paper.

Data availability

Data will be made available on request.

References

Akbari, H., Lodi, C., Muscio, A., Tartarini, P., 2021. Analysis of a new index for the thermal performance of horizontal opaque building components in summer. Atmosphere 12 (7), 862.

Akbari, H., Touchaei, A.G., 2014. Modeling and labeling heterogeneous directional reflective roofing materials. Sol. Energy Mater. Sol. Cells 124, 192–210.

ASTM, 2019. ASTM E1980-11(2019) – Standard Practice for Calculating Solar Reflectance Index of Horizontal and Low Sloped Opaque Surfaces. ASTM International, West Conshohocken, PA, USA, (2011).

Auliciems, A., 1982. Psycho-physiological criteria for global thermal zones of building design. Int. J. Biometeorol. 26 (Suppl.), 69–86.

Barrios, G., Casa, J.M., Huelsz, G., Rojas, J., 2016. Ener-habitat: An online numerical tool to evaluate the thermal performance of homogeneous and non-homogeneous envelope walls/roofs. Sol. Energy 131, 296–304.

Barrios, G., Huelsz, G., Rojas, J., Ochoa, J.M., Marincic, I., 2012. Envelope wall/roof thermal performance parameters for non airconditioned buildings. Energy Build. 50, 120–127.

Beck, H.E., Zimmermann, N.E., McVicar T.R, N., Berg, A., Wood, E.F., 2018. Present and future Köppen-Geiger climate classification maps at 1-km resolution. Sci. Data 5, 180214.

Chandra, P., 1980. Rating of wall and roof sections-thermal considerations. Build. Environ. 15 (4), 245–251.

Cheng, V., Ng, E., Givoni, B., 2013. Effect of envelope colour and thermal mass on indoor temperatures in hot humid climate. Sol. Energy 78, 528–534.

European Parliament and Council, 2002. Directive 2002/91/EC of the European parliament and of the council of 16 2002 on the energy performance of buildings (EPBD). Available online: https://eur-lex.europa.eu/.

European Parliament and Council, 2010. Directive 2010/31/EU of the European parliament and of the council of 19 2010 on the energy performance of buildings (recast) (EPBD2). Available online: https://eur-lex.europa.eu/.

European Parliament and Council, 2018. Directive (EU) 2018/844 of the European parliament and of the council of 30 2018 amending directive 2010/31/EU on the energy performance of buildings and directive 2012/27/EU on energy efficienc (EPBD3). Available online: https://eur-lex.europa.eu/.

Gasparella, A., Pernigotto, G., Baratieri, M., Baggio, P., 2011. Thermal dynamic transfer properties of the opaque envelope: Analytical and numerical tools for the assessment of the response to summer outdoor conditions. Energy Build. 43, 2509–2517.

Hong Kong Building Authority, 1995. Code of practice for overall thermal transfer value in buildings. 1995.

Hong Kong Building Department, 2014. Guidelines on design and construction requirements for energy efficiency of residential buildings.

Howell, J.R., 2022. A catalog of radiation heat transfer configuration factors – C-159: Standard standing person to rectangle on ceiling. Available online: http://www.thermalradiation.net/calc/sectionc/C-159.html.

ISO – International Organization for Standardization, 2005. ISO 7730:2005 – ergonomics of the thermal environment — Analytical determination and interpretation of thermal comfort using calculation of the PMV and PPD indices and local thermal comfort criteria (confirmed in 2015).

ISO – International Organization for Standardization, 2017. ISO 13786:2017 – thermal performance of building components - dynamic thermal characteristics — Calculation methods.

Kabre, C., 2010. A new thermal performance index for dwelling roofs in the warm humid tropic. Build. Environ. 45 (3), 727–738.

Lam, J.C., Tsang, C.L., Li, D.H.W., Cheung, S.O., 2005. Residential building envelope heat gain and cooling energy requirements. Energy 30 (7), 933–951.

Manni, M., Nicolini, A., 2021. Optimized cool coatings as a strategy to improve urban equivalent albedo at various latitudes. Atmosphere 12 (10), 1335.

Muscio, A., 2018. The solar reflectance index as a tool to forecast the heat released to the urban environment: Potentiality and assessment issues. Climate 6 (1), 12.

Muscio, A., Akbari, H., 2017. An index for the overall performance of opaque building elementssubjected to solar radiation. Energy Build. 157, 184–194.

Piselli, C., Castaldo, V.L., Pisello, A.L., 2019. How to enhance thermal energy storage effect of PCM in roofs with varying solar reflectance: Experimental and numerical assessment of a new roof system for passive cooling in different climate conditions. Sol. Energy 192, 106–119.

Pisello, A.L., Goretti, M., Cotana, F., 2012. A method for assessing buildings' energy efficiency by dynamic simulation and experimental activity. Appl. Energy 97, 419–429.

République Française, 2017. Règles th-bat – parois opaques (publié le 20 décembre 2017).

Triano-Juárez, J., Macias-Melo, E.V., Hernández-Pérez, I., Aguilar-Castro, K.M., Xamán, J., 2020. Thermal behavior of a phase change material in a building roof with and without reflective coating in a warm humid zone. J. Build. Eng. 32, 101648.